# Micelles Constructed from the Hard Core and the Shell of Symmetrically Arranged Rods. Particle Scattering Function and Mean-Square Radius of Gyration

**Masukazu Hirata and Yoshisuke Tsunashima***

*Institute for Chemical Research, Kyoto University, Uji, Kyoto-fu 611 Japan.*
*Received April 25, 1988; Revised Manuscript Received June 16, 1988*

ABSTRACT: The static light scattering behavior of highly symmetrical "sea urchin" molecules is discussed theoretically. In these molecules the inner and outer parts are constructed from the hard core and the rods of $n$ pieces arranged symmetrically in space, respectively. If the inner part is absent, they show the particle scattering function $P(q)$ and the mean-square radius of gyration $\langle S^2 \rangle$ of a regular rodlike star molecule. However, if the inner part is made invisible by using a suitable solvent, $P(q)$ shows an oscillatory dampled curve with several peaks which are characteristic of a hollow rodlike star molecule, and the apparent quantity $\langle S^2 \rangle_{app}$ differs from that of a regular rodlike star molecule. Moreover, if the inner and outer parts have different refractive indices from solvents, $P(q)$ varies from one to zero and/or to large values over unity and shows a strange oscillatory curve with several peaks and $\langle S^2 \rangle_{app}$ changes from plus infinity to minus infinity, which all depend strongly on magnitudes of the weight-fraction refractive index increments and the size ratio of the inner and outer parts of the molecules.

## Introduction

Recent developments in the static characterization of well-defined block copolymers in dilute solution by light scattering have made it possible to measure the detailed conformational nature of the intra- and intermolecular phase separation or segregation which occurs as micellar formation when the block copolymers are dissolved in a solvent that is selective for one part of the blocks. Particularly, extensive efforts have been made for *neutral* block copolymers which are constructed from some chemically different nonionic submolecules. In this case, many static properties of these copolymers in solution result from a van der Waals type of short-range interaction between two segments in the same or different submolecules and from the interaction between the segment and the solvent. Since the possible variety of the molecular structures is determined by the diversity of these interactions that emerges in the polymer–solvent system in question, the varieties that appear in such a neutral block copolymer system are not so splendid as compared with those in an *ionic* block copolymer system, where the polymers are composed of both ionic and *nonionic* submolecules. These ionic–nonionic block copolymers are amphiphiles in aqueous solution and show the properties both of neutral block copolymers and of polyelectrolytes. Various novel patterns of conformational structures are expected to be realized in aqueous solution due to the hydrophilic character of the ionic submolecules; in this system, the conformation in solution depends strongly on the degree of ionization and on the interaction between ions fixed on the polymer chain and free ions in the solutions.

In the concentration–temperature diagram for such an ionic block copolymer system,[1] it is well-known that spherical micelles, rodlike micelles, hexagonal liquid crystalline phases, or the hydrated solid are formed, depending on how the solution concentration and temperature are far from the critical micellar concentration (cmc) and temperature. Moreover, the cmc is usually extremely low;[2] i.e., molecular dispersion of ionic block copolymers in solution is very hard to realize. All of these features are rarely observed for neutral block copolymers in organic solvents.[3] In salt-free aqueous solutions of ionic–nonionic block copolymers, the electrostatic repulsions between ionized submolecules are very strong. It is thus plausible that the copolymers form a spherical micelle which is composed of a collapsed hydrophobic core with a number of hydrophilic submolecules (rays) extended outward radially. No conformational study on this type ("sea urchin" like) of micelle has been done so far, though it will give us wider and deeper insight into the intra- and intermolecular characteristics which appear in various forms of micelles. In fact, very recently, we have succeeded in preparation of salt-free aqueous solution of amphiphilic diblock copolymers by synthesizing poly(*N*-ethyl-2-vinylpyridinium)-*block*-polystyrene and observed the micellar formation of a sea urchin type in high probability.[4] We therefore investigate in the present paper the typical static characteristics in solution, i.e., the particle scattering function and the mean-square radius of gyration, of the sea urchin type of molecule. Here the molecule is represented by a model which is constructed from a rigid spherical "core" and an outer "shell" of $n$ spatially symmetrically arranged thin rods. This model is reduced to a rodlike star molecules when the inner core becomes infinitesimmally small. A hollow rodlike star molecules is also realized if the core can be made invisible by choosing a solvent that matches its refractive index.

## Particle Scattering Function

For rigid molecules, the relative positions between different segments are fixed. Let $\mathbf{R}_{jk}$ be the distance between the $j$th and the $k$th segments in a molecule that is oriented to a given direction against the scattering vector $\mathbf{q}$. The particle scattering function for the molecules $P(q)$ is given by

$$P(q) = N^{-2}\sum_{j=1}^{N}\sum_{k=1}^{N}\langle \exp(i\mathbf{q}\cdot\mathbf{R}_{jk})\rangle \qquad (1)$$

with $\langle\ \rangle$ the configurational average over all the orientation of the molecule and $N$ the total number of segments composed of the molecules. $P(q)$ is normalized to unity at $\mathbf{q} = 0$. Averaged over all the orientation of $\mathbf{R}_{jk}$ to $\mathbf{q}$, the $P(q)$ can be obtained as

$$P(q) = N^{-2}\sum_{j=1}^{N}\sum_{k=1}^{N}\sin(qR_{jk})/qR_{jk}, \qquad R_{jk} = |\mathbf{R}_k - \mathbf{R}_j| \qquad (2)$$

As shown in Figure 1, the sea urchin molecule is composed of two parts, an inner rigid core of radius $r_c$ and an outer shell of $n$ radially arranged rods of length $L$. The $P(q)$ can then be expressed by a following summation

$$P(q) = [w_i^2\nu_i^2P_i(q) + w_o^2\nu_o^2P_o(q) + 2w_iw_o\nu_i\nu_oP_{io}(q)]/(w_i\nu_i + w_o\nu_o)^2 \qquad (3)$$

0024-9297/89/2222-0249$01.50/0 

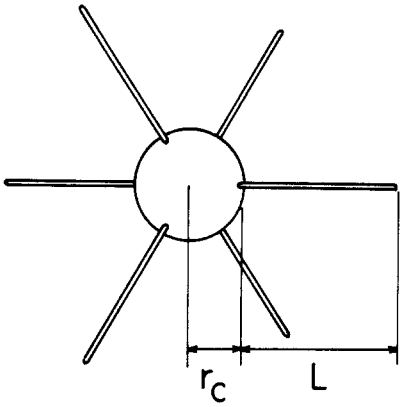


**Figure 1.** Model of a sea urchin molecule. The core radius is $r_c$ and the lengths of $n$ rods are all $L$.

In this equation, $P_i(q)$, $P_o(q)$, and $P_{io}(q)$ are the *partial* particle scattering function for the inner core, the outer shell rods, and the interference between the core and the shell, respectively. The quantity $(w_i\nu_i + w_o\nu_o)$ represents the refractive index increment of the whole molecule with $w_t$ and $\nu_t$ the weight fraction and the refractive index increment of the t (t = i and o) part, respectively. $P_i(q)$ is given by the particle scattering function for the hard sphere[5] of radius $r_c$

$$P_i(q) = (3/x^3)^2(\sin x - x\cos x)^2$$

$$x = qr_c = (5/3)^{1/2}q\langle S^2\rangle_i^{1/2} \qquad \text{(sphere)} \qquad (4)$$

where $\langle S^2\rangle_i$ is the mean-square radius of gyration of the sphere. The other particle scattering functions $P_o(q)$ and $P_{io}(q)$ can be obtained in the following way.

**Particle Scattering Function of the Outer Shell Rods $P_o(q)$.** Consider that $n$ rods of length $L$ are distributed in space with regularity. Let $N_o$ be the total number of segments of $n$ rods, and divide $N_o$ into $n$ subparts of equal number of segments $N_o/n$; each rod contains $N_o/n$ segments. $P_o(q)$ can then be expressed by sum of $n^2$ *partial* particle scattering functions $P_o(q,l,m)$ as follows

$$P_o(q) = N_o^{-2}\sum_{j=1}^{N_o}\sum_{k=1}^{N_o}(\sin qR_{jk})/qR_{jk} = n^{-2}\sum_{l=1}^{n}\sum_{m=1}^{n}P_o(q,l,m) \qquad (5)$$

$$P_o(q,l,m) = (N_o/n)^{-2}\sum_{j(l)=1}^{N_o/n}\sum_{k(m)=1}^{N_o/n}\sin qR_{j(l)k(m)}/qR_{j(l)k(m)} \qquad (6)$$

Here $P_o(q,l,m)$ denotes the interference due to all pairs of the segments on the $l$th and $m$th rod, e.g., $j$ on the $l$th rod and $k$ on the $m$th rod. $R_{j(l)k(m)}$ represents the magnitude of the distance between this two segments, which are located in the spatial positions $\mathbf{R}_{j(l)}$ and $\mathbf{R}_{k(m)}$, respectively. For $l = m$, $P_o$ becomes the intrarod interference and the $P_o(q,l,l)$ values are all equal to each other for $l = 1$–$n$. For $l \neq m$, $P_o$ is the interrod interference with $P_o(q,l,m) = P_o(q,m,l)$. Since the $l$th and $m$th rods are fixed in space, we can specify the absolute positions of the start and end points for each rod to be $\mathbf{S}_{l1}$ and $\mathbf{S}_{l2}$ for the rod $l$ and $\mathbf{S}_{m1}$ and $\mathbf{S}_{m2}$ for the rod $m$. Then we have

$$R_{j(l)k(m)} = Lr(s_j,s_k)$$

$$r(s_j,s_k) = |[(1 - s_j)\mathbf{S}_{l1} + s_j\mathbf{S}_{l2}] - [(1 - s_k)\mathbf{S}_{m1} + s_k\mathbf{S}_{m2}]|/L \qquad (7)$$

where $s_j$ and $s_k$ are the relative positions ($0 \le s_t \le 1$, $t = j, k$) of the $j$th and $k$th segments on the $l$th and $m$th rods, measured from each start segment, respectively. The $P_o(q)$ expression in eq 5, together with eq 6 and 7, is general in form and is applicable to every case where rods are distributed in space with some regularity. Generally, the evaluation of $P_o(q)$ is very tedious because $P_o(q)$ depends strongly on the relative orientations of a given pair of $l$th and $m$th rods. However, it becomes simpler in the present sea urchin type of molecules since the rods are arranged highly symmetrically.

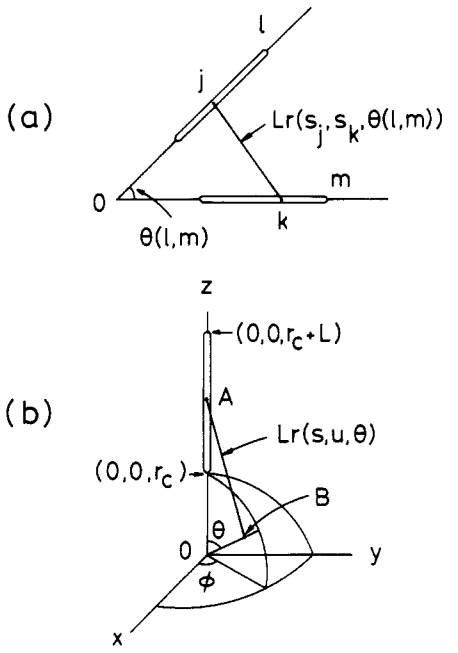


**Figure 2.** Spatial geometry on the interference (a) between two rods and (b) between a rod and the core.

When the molecular center is set in the origin of the coordinate, each rod in the model is arranged on the radial lines directed from the origin to the vertexes of regular polyhedrons or to the face centers of pseudoregular polyhedrons, of which centers are also set on the origin. The one end of each rod is put on an intersection of the radial line with the spherical core surface and another end is set on a vertex of the polyhedron or a face center of the pseudopolyhedron (Figure 2a). Let $\theta(l,m)$ be the spatial angle between the $l$th and $m$th rods; it follows that

$$|\mathbf{S}_{l1}| = |\mathbf{S}_{m1}| = r_c$$

$$[(\mathbf{S}_{l2} - \mathbf{S}_{l1})\cdot(\mathbf{S}_{m2} - \mathbf{S}_{m1})]/L^2 = \cos\theta(l,m)$$

$P_o(q,l,m)$ in eq 6 can then be classified into several subgroups, so that, in each subgroup $t$, all the angles $\theta(l,m)$ should be equal to $\theta_t$, independent of $l$ and $m$, and that all the $P_o(q,l,m)$s should give a same value depending only on $\theta_t$. If we have $d$ blocks of these subgroups and each subgroup contains $c_t$ pieces of equivalent $P_o(q,l,m)$, we can rewrite eq 5–7 as

$$P_o(q) = n^{-2}[nP_o(q,l,l) + 2_nC_2P_o(q,l,m;l<m)] = n^{-2}[nP_o(q,l,l) + \sum_{t=1}^{d}c_tP_o(q,\theta_t)] \qquad (8)$$

$$r(s_j,s_k) = [(s_j + r_c/L)^2 + (s_k + r_c/L)^2 - 2(s_j + r_c/L)(s_k + r_c/L)\cos\theta_t]^{1/2} \equiv r(s_j,s_k,\theta_t) \qquad (9)$$

with

$$\sum_{t=1}^{d}c_t = 2_nC_2 = n(n-1) \qquad (10)$$

In eq 8, the first term is a contribution due to the intrarod interference and becomes $nP_o(q,l,l) = c_0P_o(q,\theta_0)$ with $c_0 =$

Table I
Values of $d$, $c_t$, and cos $\theta_t$ in Classified *Partial* Particle Scattering Functions, $P_o(q,\theta_t)$, for the Sea Urchin Shell of $n$ Rods

| $n$ | $d$ | $t$ | $c_t$ | cos $\theta_t$ |
|---|---|---|---|---|
| 2 | 1 | 0 | 2 | 1 |
| | | 1 | 2 | −1 |
| 3 | 1 | 0 | 3 | 1 |
| | | 1 | 6 | −1/2 |
| 4 | 1 | 0 | 4 | 1 |
| | | 1 | 12 | −1/3 |
| 6 | 2 | 0 | 6 | 1 |
| | | 1 | 24 | 0 |
| | | 2 | 6 | −1 |
| 8 | 3 | 0 | 8 | 1 |
| | | 1 | 24 | 1/3 |
| | | 2 | 24 | −1/3 |
| | | 3 | 8 | −1 |
| 12 | 3 | 0 | 12 | 1 |
| | | 1 | 60 | $1/5^{1/2}$ |
| | | 2 | 60 | $-1/5^{1/2}$ |
| | | 3 | 12 | −1 |
| 20 | 5 | 0 | 20 | 1 |
| | | 1 | 60 | $5^{1/2}/3$ |
| | | 2 | 120 | 1/3 |
| | | 3 | 120 | −1/3 |
| | | 4 | 60 | $-5^{1/2}/3$ |
| | | 5 | 20 | −1 |
| 32 | 11 | 0–11 | $a$ | $a$ |
| 92 | 53 | 0–53 | $a$ | $a$ |

[a] Evaluations of these values were made by a computer algorithm under the symmetricity check of $n$ rods. The results were not shown here because there are too many $t$'s to list.

$n$ and $\theta_0 = 0$, and the second term $P_o(q,\theta_t)$ represents the interrod *partial* particle scattering function. Then eq 8 becomes

$$P_o(q) = n^{-2}\sum_{t=0}^{d} c_t P_o(q,\theta_t) \tag{11}$$

$$P_o(q,\theta_t) = (N_o/n)^{-2}\int_0^1\int_0^1[\sin qLr(s_j,s_k)/qLr(s_j,s_k)] \times [(N_o/n)/L]^2\, d(Ls_j)\, d(Ls_k) = \int_0^1\int_0^1[\sin qLr(s_j,s_k,\theta_t)/qLr(s_j,s_k,\theta_t)]\, ds_j\, ds_k \tag{12}$$

Considering the spatial symmetry, we take the following number of rods $n$ for the sea urchin molecules: $n$ = 2, 3, 4, 6, 8, 12, 20, 32, and 92. In the cases of $n$ = 2 and 3, the rods are arranged in plane with the interrod angles 180° and 120°, respectively, and are strictly not in spatial symmetry. The others are, however, all in spatial symmetry; the case of $n$ = 4 corresponds to a tetrahedron, 6 to an octahedron, 8 to a cube, 12 to an icosahedron, and 20 to a dodecahedron. The case of $n$ = 32 results from the superposition of the case of $n$ = 12 with that of $n$ = 20, and the case of $n$ = 92 results from the insertion of a new piece of rod into each center of a triangle which is constructed by the nearest three rods in the case of $n$ = 32. For all these cases, the values of $d$, $c_t$, and cos $\theta_t$ were examined for each classified $P_o(q,\theta_t)$ and the results are summarized in Table I. Evaluation of the $P_o(q,\theta_t)$, i.e., the integration of eq 12, was pursued numerically through the two-dimensional Simpson's $^1/_3$ rule, where the integration intervals were divided equally into 128 parts. The computation was made by a FACOM M-380Q computer in our institute.

**Particle Scattering Function Due to Interaction between the Core and Shell Rods $P_{io}(q)$.** Since every rod is in the equivalent position relative to the spherical core in the present model, $P_{io}(q)$ can be obtained from the interference between a rod and the core and is independent of $n$. Let the rod be set on the $z$ axis of the spherical coordinates and select two segments each from the rod and the inner core (Figure 2b); one is located at $A(0, 0, r_c + sL)$ on the rod with $0 \le s \le 1$ and another at $B(uL \sin\theta \cos\phi, uL \sin\theta \sin\phi, uL \cos\theta)$ in the core with $uL$ the radial distance ($0 \le u \le r_c/L$) and $\theta$ and $\phi$ the usual Euler's angles ($0 \le \theta \le \pi$, $0 \le \phi \le 2\pi$). The distance between the two points is given by

$$Lr(s,u,\theta) = L[u^2 + (s + r_c/L)^2 - 2u(s + r_c/L)\cos\theta]^{1/2} \tag{13}$$

Let $N_i$ be the number of segments in the core. The interference term $P_{io}(q)$ between the core with $N_i$ segments and the rod with $N_o/n$ segments is expressed by the following integral

$$P_{io}(q) = N_i^{-1}(N_o/n)^{-1}\int_0^1\int_0^\pi\int_0^{r_c/L}[\sin qLr(s,u,\theta)/qLr(s,u,\theta)][2\pi N_i L^3 u^2\, du \sin\theta\, d\theta/(4\pi r_c^3/3)] \times [(N_o/n)/L]\, d(sL) = (3/2)(r_c/L)^{-3} \times \int_0^1\int_0^\pi\int_0^{r_c/L}[\sin qLr/qLr]u^2 \sin\theta\, du\, d\theta\, ds \tag{14}$$

at $r_c > 0$. The evaluation of eq 14 was again carried out numerically by the computer as described above.

## Mean-Square Radius of Gyration

The apparent mean-square (ms) radius of gyration for the sea urchin molecules $\langle S^2\rangle_{app}$ is expressed by

$$\langle S^2\rangle_{app} = [w_i^2\nu_i^2\langle S^2\rangle_i + w_o^2\nu_o^2\langle S^2\rangle_o + 2w_iw_o\nu_i\nu_o\langle S^2\rangle_{io}]/(w_i\nu_i + w_o\nu_o)^2 \tag{15}$$

where $\langle S^2\rangle_i$, $\langle S^2\rangle_o$, and $\langle S^2\rangle_{io}$ are the *partial* ms radius of gyration due to the core, the shell, and the cross term between them, respectively. In general, the ms radius of gyration $\langle S^2\rangle$ can be estimated by

$$\langle S^2\rangle = -3(dP(q)/dq^2)_{q=0} \tag{16}$$

Here we use an expression that $\sin x/x = 1 - x^2/3! + x^4/5! + \ldots$ Thus $\langle S^2\rangle_o$ can be obtained from eq 11 and 12 as

$$\langle S^2\rangle_o = n^{-2}\sum_{t=0}^{d} c_t\langle S^2(\theta_t)\rangle_o \tag{17}$$

with

$$\langle S^2(\theta_t)\rangle_o = (L^2/2)\int_0^1\int_0^1 r^2(s_j,s_k,\theta_t)\, ds_j\, ds_k \tag{18}$$

Substitution of eq 9 into eq 18 gives that

$$\langle S^2(\theta_t)\rangle_o = L^2[\{1/3 + r_c/L + (r_c/L)^2\} - \{1/4 + r_c/L + (r_c/L)^2\}\cos\theta_t] \tag{19}$$

and eq 17 becomes

$$\langle S^2\rangle_o = [1/3 + r_c/L + (r_c/L)^2]L^2 \tag{20}$$

since $n^{-2}\sum_{t=0}^{d} c_t = 1$ and $\sum_{t=0}^{d} c_t \cos\theta_t = 0$ due to the spatial symmetry of the present molecules (Table I). $\langle S^2\rangle_{io}$ can be obtained similarly from eq 13 and 14 as

$$\langle S^2\rangle_{io} = (L^2/2)(3/2)(r_c/L)^{-3}\int_0^1\int_0^\pi\int_0^{rc/L} r^2(s,u,\theta)u^2 \times \sin\theta\, du\, d\theta\, ds = [1/6 + r_c/2L + (4/5)(r_c/L)^2]L^2 \tag{21}$$

For the rigid sphere of radius $r_c$, it follows that

$$\langle S^2\rangle_i = (3/5)r_c^2 \tag{22}$$

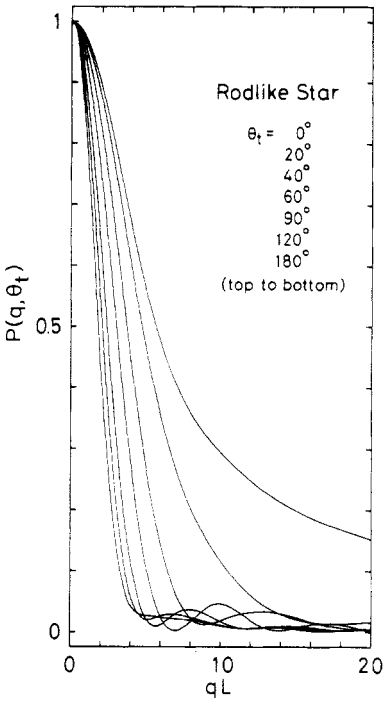


**Figure 3.** Partial particle scattering function $P(q,\theta_t)$ for rodlike star molecules at a given angle between the $l$th and $m$th rods $\theta_t$ $(=\theta(l,m)$ in Figure 2a.

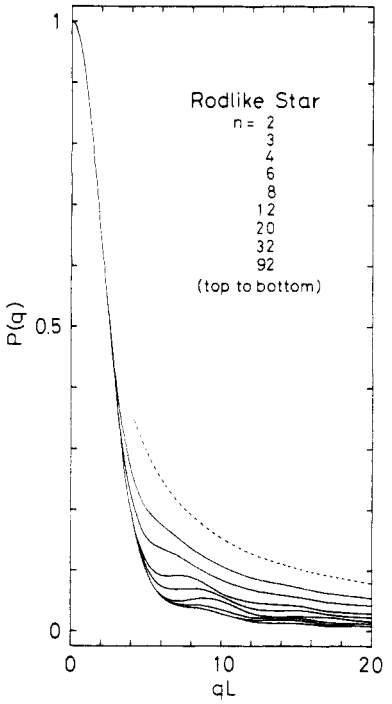


**Figure 4.** Particle scattering function for rodlike star molecules $P(q)$ with $n$ rods. A broken curve represents $n = 2$ and the other real curves $n$ = 3–92.

With eq 20–22, we can estimate from eq 15 the values of $\langle S^2\rangle_{app}$ for the sea urchin molecules of given $w_t$ and $\nu_t$ ($t$ = i and o).

## Results and Discussion

In what follows, we first discuss the results on the $q$ dependences of *partial* particle scattering functions $P_o(q)$ and $P_{io}(q)$ and then on the variation of whole molecular values $P(q)$ and $\langle S^2\rangle$ with $w_t$ and $\nu_t$ for the sea urchin molecules.

***P(q)* for Rodlike Star Molecules.** For the star molecules of $n$ rods (abbreviated as RS$n$), the central hard

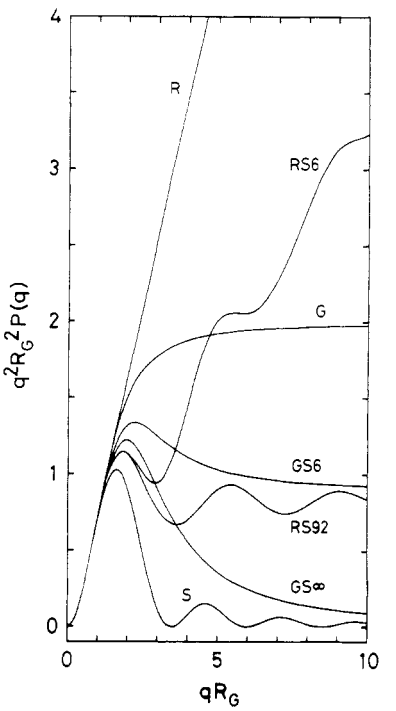


**Figure 5.** Kratky plots for various types of molecules: RS$n$, rodlike stars (present work); R, rods; G, Gaussian coils; GS$n$, regular stars of $n$ Gaussian subchains; S, spheres.

core of sea urchin molecules does not exist and the $P_o(q,\theta_t)$ and $P_o(q)$ at $r_c/L = 0$ become the whole molecular values $P(q,\theta_t)$ and $P(q)$. In Figure 3, the $P(q,\theta_t)$ is plotted against $qL$ with changing $\theta_t$ from 0° to 180° discretely. At first, it is found that the values of $P(q,\theta_t)$ are positive in any case. This means that $P(q)$ has always positive values. Second, some peaks appear at $\theta_t > 40°$ in the dampled oscillatory forms. The amplitudes and positions depend strongly on $\theta_t$, though the former are less than 0.05 in the magnitude. Table II shows the $P(q)$ values as a function of $qL$ for all $n$ described above. These values are always positive and are plotted in Figure 4 against $qL$ for $n$ = 2–92. A broken curve for $n = 2$ represents $P(q)$ for a rod of length $2L$. Usually, the $P(q)$ curves decrease sharply at small $qL$, then damp with oscillation, and finally reach zero as $qL$ increases. Several peaks are detectable at $qL > 5$ for $n \geq 3$. This $P(q)$ feature for RS$n$ molecules is graphically compared in Figure 5 with the $P(q)$ for other particular shaped molecules. Here the Kratky plot, i.e., $q^2R_G^2P(q)$ vs $qR_G$, is employed with $R_G$ the root ms radius of gyration of the whole molecule. The molecules examined are rods of length $L'$ (curve R),[6] Gaussian coils (curve G),[7] regular stars of $n$ Gaussian subchains each having the same radius of gyration $R_G'$ (curve GS$n$),[8] and spheres (curve S). These $P(q)$s were calculated by the following equations:

$$P(q) = x^{-1}\int_0^{2x}(\sin x/x)\,dz - (\sin x/x)^2,$$
$$x = qL'/2 = 3^{1/2}qR_G \quad \text{(rod)}$$

$$P(q) = (2/x^2)[\exp(-x) - 1 + x],$$
$$x = (qR_G)^2 \quad \text{(Gaussian coils)}$$

$$P(q) = (2/nx)[x - \{1 - \exp(-x)\} + \{(n-1)/2\}\{1 - \exp(-x)\}^2], \quad x = n(3n-2)^{-1}(qR_G)^2 = (qR_G')^2 \quad \text{(GS}n\text{)}$$

$$P(q) = \text{see Table II},$$
$$qL = 3^{1/2}qR_G \quad \text{(this work)} \quad \text{(RS}n\text{)}$$

Due to the high intramolecular symmetry, the plotted curves of RS$n$ and S show the characteristic oscillatory

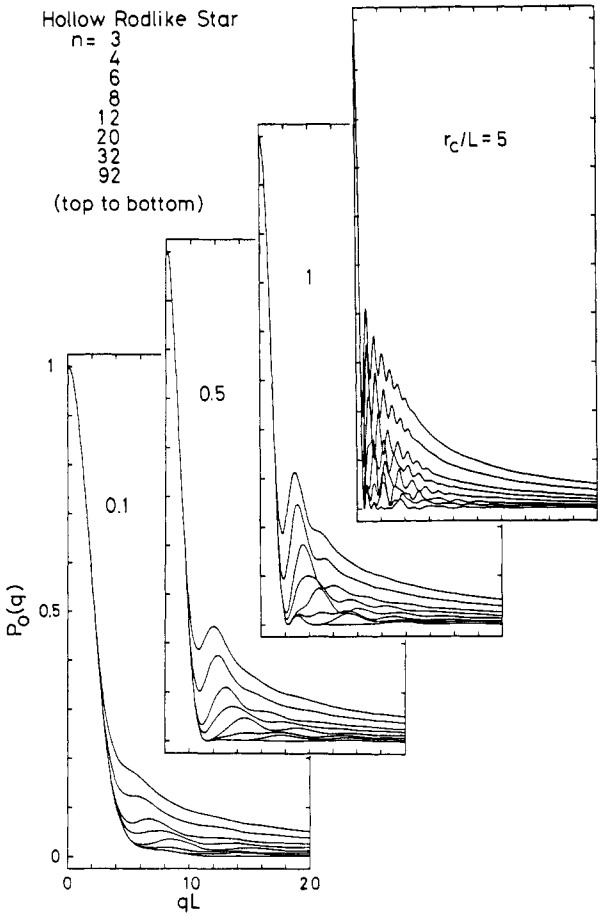


**Figure 6.** Particle scattering function for hollow rodlike star molecules $P_o(q)$ with $n$ rods. The core to shell size ratio $r_c/L$ is taken to be 0.1, 0.5, 1, and 10. In each subfigure, the eight curves represent $P_o(q)$ for $n$ = 3, 4, 6, 8, 12, 20, 32, and 92 from top to bottom.

behavior over the wide range of $qR_G$. Especially at $qR_G$ larger than 1.8, RS$n$ curves reveal their distinct characteristics from those of other shapes of molecules. The number $n$ for RS$n$ will be detectable if the $P(q)$ data are obtained at higher $qR_G$, say, more than 4.

***P*(*q*) for Hollow Rodlike Star Molecules.** In this case, the molecules are exactly the "shell" of sea urchin molecules where the "core" is made invisible optically. The typical $P_o(q)$ curves are shown in Figure 6 as a function of $qL$ for four cases of $r_c/L$ = 0.1, 0.5, 1, and 5, respectively. In each sub-Figure where $r_c/L$ is fixed, the number of rods $n$ is changed as $n$ = 3, 4, 6, 8, 12, 20, 32, and 92, from the top to the bottom. It is found that the oscillatory feature in $P_o(q)$ becomes clear as $r_c/L$ increases; at a constant $n$, the $P_o(q)$ gives larger peak height and lower peak position (in terms of $qL$) with increasing $r_c/L$. This feature is responsible to the situations that, with increasing $r_c$, the distance between a pair of rods spreads enough to show some detectable periodicity.

**Interference Term between the Core and the Shell, $P_{io}(q)$.** Figure 7 shows $P_{io}(q)$ for sea urchin molecules as a function of $qL$. As described already, $P_{io}(q)$ is independent of $n$ and varies with a parameter $r_c/L$. The value of $r_c/L$ was changed as 0.001, 0.1, 0.2, 0.5, 1, 2, 5, and 10, as indicated in Figure 7. At $r_c/L < 0.2$, the $P_{io}(q)$ gives detectable damped oscillatory curves which reach zero asymptotically from the positive region, but at $r_c/L > 0.5$ it decreases quickly to the negative region and then turns back to zero within a comparably small range of $qL$. The former is a distinct characteristic of the sea urchin molecules with high intramolecular symmetry. Moreover,

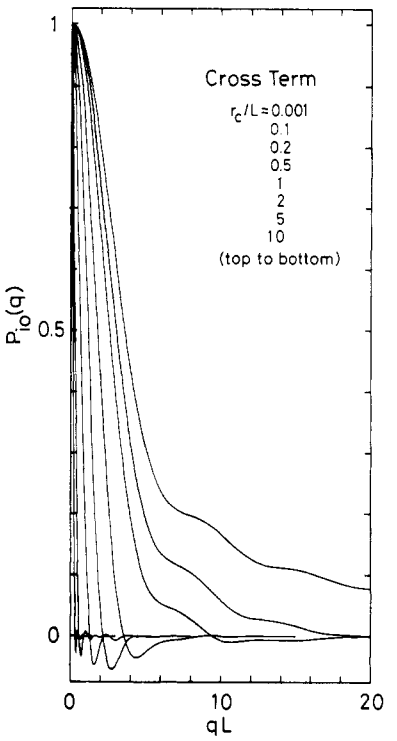


**Figure 7.** Particle scattering function due to the interference between the core and the shell $P_{io}(q)$ for sea urchin molecules with a given size ratio $r_c/L$.

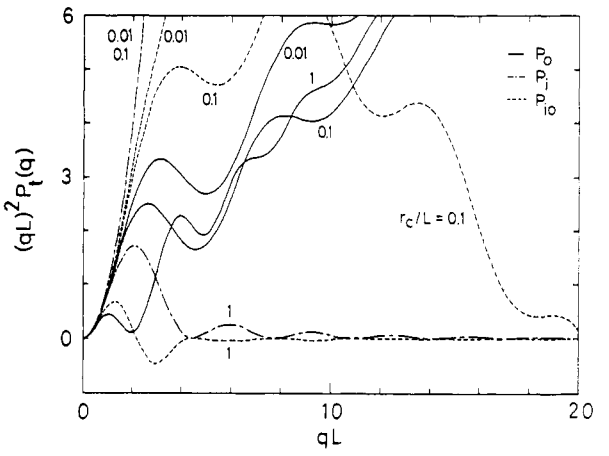


**Figure 8.** Kratky plots for three components of the sea urchin molecules with $r_c/L$ = 0.01, 0.1, and 1. $P_o$ (—) represents the curve for the hollow rodlike star part of $n$ = 6, $P_i$ (- - -) for the core part, and $P_{io}$ (- · -) for the core–shell interference part. For $P_i$, the core size $r_c$ was expressed in terms of $qL$ with the relation $qr_c = qL(r_c/L)$.

Figure 7 indicates that the interference effect becomes negligibly small when the core size $r_c$ becomes larger than a quarter of the rod length.

***P*(*q*) for Sea Urchin Molecules.** Figure 8 shows, as an example, the Kratky plots, $(qL)^2P_t(q)$ vs $qL$, of three components ($t$ = o, io, and i) of $P(q)$, i.e., $P_o(q)$ for hollow rodlike stars of six arms, $p_{io}(q)$ for core–shell interactions, and $P_i(q)$ for cores, respectively. In each case, the molecular size was indicated by the ratio $r_c/L$ and it was changed as 0.01, 0.1, and 1 as indicated by the figures on the curves. Each curve reveals clearly the oscillatory behavior and shows no plateau constant in larger $qL$, which is characteristic of the Gaussian chains. Since $P(q)$ for sea urchin molecules can be evaluated from eq 3, the $P(q)$ structure depends strongly on $w_t$ and $\nu_t$ of the core ($t$ = i) and the shell ($t$ = o) parts of the molecules and as well

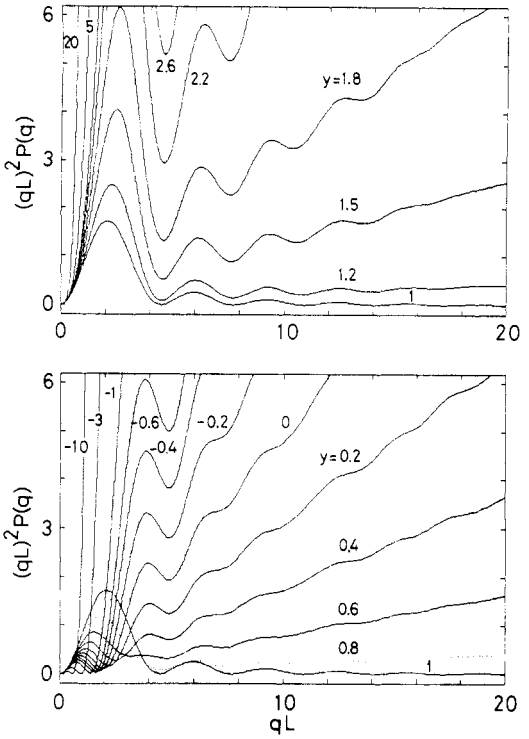


**Figure 9.** Kratky plots for sea urchin molecules with $n = 6$ and $r_c/L = 1$. The weight-fraction refractive index increment of the core part $y$ is changed from 20 to −10 as indicated by figures on the curve.

as on $r_c/L$. The size ratio $r_c/L$ depends on $w_i$. For example, if the molecules are diblock copolymers, it follows that

$$r_c/L = n^{1/3}[w_i^{1/3}/(1 - w_i)][M/(4\pi d_i/3)]^{1/3}/(M/d_o) = [(nw_i)^{1/3}/(1 - w_i)](R^*/L^*) \quad (23)$$

where $M$ is the molecular weight of a single block copolymer, $d_i$ the density of the core, and $d_o$ the density of the rod per unit length. $R^*$ and $L^*$ represent the molar equivalent sphere radius of the core part and the molar length of the shell part of the block copolymer, respectively. When the weight-fraction refractive index increment of the core part $y$ defined by[9]

$$y = w_i\nu_i/(w_i\nu_i + w_o\nu_o) \quad (24)$$

is introduced, the $y$ becomes a variable changing from $+\infty$ to $-\infty$ and is independent of $r_c/L$. $P(q)$ of eq 3 then becomes a function of $y$ and $r_c/L$ alone:

$$P(q) = y^2P_i(q) + (1 - y)^2P_o(q) + 2y(1 - y)P_{io}(q) \quad (25)$$

For eq 25, three special cases can be considered: (1) the core part actually *disappears*, or solvents are chosen so that (2) the *core part* should be made *invisible* or that (3) the *total* refractive index increment of the polymer should be zero, i.e., $w_i\nu_i + w_o\nu_o = 0$. The first case is the rodlike star micelles where $w_i = 0$ ($y = 0$) and $r_c/L = 0$, and $P(q) = P_o(q)_{r_c=0}$, as shown already in Figure 4. The second case gives hollow rodlike star micelles where $\nu_i = 0$ ($y = 0$) and $r_c/L \neq 0$, and the $P(q)$ is given by $P(q) = P_o(q)_{r_c\neq 0}$ and is illustrated already in Figure 6. In the third case where $y = \pm\infty$, no light is scattered at zero angle but the characteristic scattered light can be observed at finite angles; in the very small $qL$ region, the $P(q)$ continues to increase with $qL$ from 1 to a large positive value in the case $y = +\infty$, while it decreases at first and then increases up to a large positive value with a sharp minimum in the case $y = -\infty$. Even in other usual cases where $-A < y < A$ ($A$ = positive value), the $P(q)$ estimated from eq 25 still shows strange and complex behavior of oscillatory character. The strange behavior is caused mainly by the magnitudes of outer shell contribution $P_o(q)$ and of cross-term contribution $P_{io}(q)$, as demonstrated in Figure 8. The characteristic behavior described here will be show in detail in Figures 9–11.

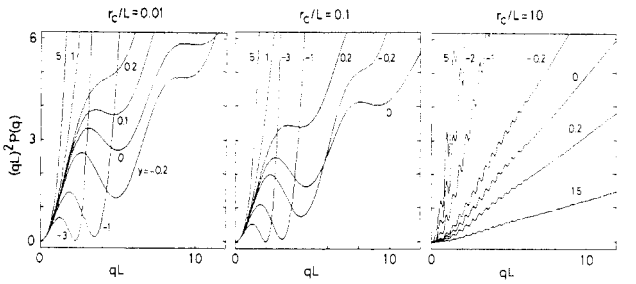


**Figure 10.** Same plots as in Figure 9 but for $r_c/L = 0.01$, 0.1, and 10. The number of rods is 6.

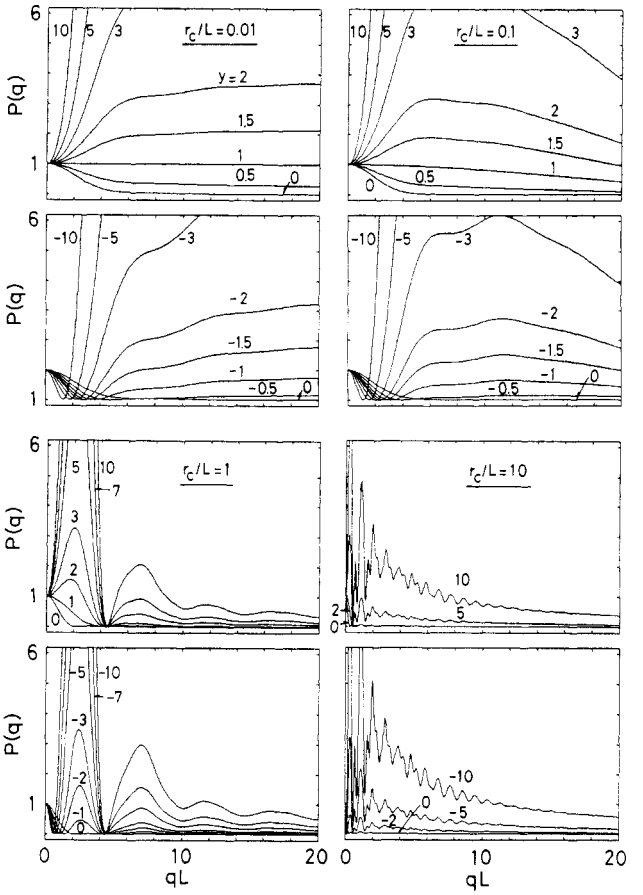


**Figure 11.** Plots of the particle scattering function $P(q)$ against $qL$ for sea urchin molecules with $n = 32$. Four cases of $r_c/L = 0.01$, 0.1, 1, and 10 are shown by a pair of subfigures ($y \geq 0$ and $y \leq 0$) from the top left to the bottom right.

Figure 9 shows an example of the $(qL)^2P(q)$ vs $qL$ plots for sea urchin molecules with $n = 6$ at $r_c/L = 1$. Here, the parameter $y$ was changed from negative to positive values as indicated by the figures on the curves. At $y > 1$, $(qL)^2P(q)$ shows several peaks which decrease both in the heights and in the initial slopes (at $qL = 0$) with decreasing $y$. At $y < 1$, the first peak decreases both in height and in the $qL$ position but the second and other peaks increase in height with decreasing $y$. Especially the change in $(qL)^2P(q)$ at small $qL$, $0 < qL < 2$, is very drastic when $y$ is in the region $-1 < y < 1$. These will be revealed later in the $y$ dependence of $\langle S^2\rangle_{app}$. Similar plots are also shown in Figure 10 with changing $r_c/L$ as 0.01, 0.1, and 10. Here $n = 6$ and $y$ was restricted around $-1 < y < 1$. At

Table II
Values of $P(q)$ for Rodlike Star Molecules of $n$ Rays as a Function of $qL$ and $n$

| | n | | | | | | | | |
|---|---|---|---|---|---|---|---|---|---|
| qL | 2 | 3 | 4 | 6 | 8 | 12 | 20 | 32 | 92 |
| 0.00 | 1.000 00 | 1.000 00 | 1.000 00 | 1.000 00 | 1.000 00 | 1.000 00 | 1.000 00 | 1.000 00 | 1.000 00 |
| 0.50 | 0.972 77 | 0.972 66 | 0.972 62 | 0.972 62 | 0.972 62 | 0.972 62 | 0.972 62 | 0.972 62 | 0.972 62 |
| 1.00 | 0.897 34 | 0.895 66 | 0.895 09 | 0.895 07 | 0.895 07 | 0.895 07 | 0.895 07 | 0.895 07 | 0.895 07 |
| 1.50 | 0.790 21 | 0.782 72 | 0.780 12 | 0.779 91 | 0.779 91 | 0.779 91 | 0.779 91 | 0.779 91 | 0.779 91 |
| 2.00 | 0.672 40 | 0.652 52 | 0.645 41 | 0.644 38 | 0.644 36 | 0.644 34 | 0.644 34 | 0.644 34 | 0.644 34 |
| 2.50 | 0.562 67 | 0.524 00 | 0.509 58 | 0.506 34 | 0.506 21 | 0.506 10 | 0.506 10 | 0.506 10 | 0.506 10 |
| 3.00 | 0.472 68 | 0.412 03 | 0.388 28 | 0.380 58 | 0.380 11 | 0.379 73 | 0.379 72 | 0.379 72 | 0.379 72 |
| 3.50 | 0.405 55 | 0.324 89 | 0.291 46 | 0.276 68 | 0.275 37 | 0.274 33 | 0.274 32 | 0.274 31 | 0.274 31 |
| 4.00 | 0.357 75 | 0.263 89 | 0.222 46 | 0.198 55 | 0.195 62 | 0.193 25 | 0.193 22 | 0.193 20 | 0.193 20 |
| 4.50 | 0.322 82 | 0.224 98 | 0.178 89 | 0.145 42 | 0.139 81 | 0.135 27 | 0.135 17 | 0.135 12 | 0.135 12 |
| 5.00 | 0.294 89 | 0.201 44 | 0.154 67 | 0.113 39 | 0.104 10 | 0.096 51 | 0.096 22 | 0.096 09 | 0.096 09 |
| 5.50 | 0.270 51 | 0.186 50 | 0.142 53 | 0.097 15 | 0.083 54 | 0.072 29 | 0.071 61 | 0.071 31 | 0.071 31 |
| 6.00 | 0.248 66 | 0.175 13 | 0.136 04 | 0.091 14 | 0.073 37 | 0.058 40 | 0.057 00 | 0.056 38 | 0.056 38 |
| 6.50 | 0.229 58 | 0.164 64 | 0.130 86 | 0.090 44 | 0.069 59 | 0.051 56 | 0.048 99 | 0.047 85 | 0.047 85 |
| 7.00 | 0.213 51 | 0.154 26 | 0.124 87 | 0.091 15 | 0.069 13 | 0.049 34 | 0.045 08 | 0.043 19 | 0.043 19 |
| 7.50 | 0.200 12 | 0.144 27 | 0.117 73 | 0.090 70 | 0.069 77 | 0.049 86 | 0.043 45 | 0.040 59 | 0.040 58 |
| 8.00 | 0.188 62 | 0.135 10 | 0.109 99 | 0.087 86 | 0.069 97 | 0.051 55 | 0.042 70 | 0.038 75 | 0.038 73 |
| 8.50 | 0.178 25 | 0.126 92 | 0.102 39 | 0.082 60 | 0.068 85 | 0.053 05 | 0.041 85 | 0.036 82 | 0.036 77 |
| 9.00 | 0.168 64 | 0.119 56 | 0.095 37 | 0.075 72 | 0.066 06 | 0.053 35 | 0.040 26 | 0.034 36 | 0.034 25 |
| 9.50 | 0.159 79 | 0.112 74 | 0.089 07 | 0.068 38 | 0.061 72 | 0.051 90 | 0.037 76 | 0.031 32 | 0.031 09 |
| 10.00 | 0.151 86 | 0.106 33 | 0.083 41 | 0.061 61 | 0.056 29 | 0.048 65 | 0.034 53 | 0.027 96 | 0.027 53 |
| 10.50 | 0.144 88 | 0.100 39 | 0.078 32 | 0.056 05 | 0.050 41 | 0.044 03 | 0.030 97 | 0.024 68 | 0.023 91 |
| 11.00 | 0.138 65 | 0.095 14 | 0.073 84 | 0.051 88 | 0.044 77 | 0.038 75 | 0.027 57 | 0.021 84 | 0.020 61 |
| 11.50 | 0.132 94 | 0.090 74 | 0.070 07 | 0.048 96 | 0.039 98 | 0.033 59 | 0.024 75 | 0.019 72 | 0.017 85 |
| 12.00 | 0.127 56 | 0.087 16 | 0.067 08 | 0.046 98 | 0.036 45 | 0.029 19 | 0.022 73 | 0.018 38 | 0.015 74 |
| 12.50 | 0.122 49 | 0.084 20 | 0.064 80 | 0.045 63 | 0.034 29 | 0.025 93 | 0.021 54 | 0.017 76 | 0.014 27 |
| 13.00 | 0.117 79 | 0.081 55 | 0.063 01 | 0.044 64 | 0.033 34 | 0.023 91 | 0.021 04 | 0.017 65 | 0.013 31 |
| 13.50 | 0.113 51 | 0.078 94 | 0.061 40 | 0.043 80 | 0.033 20 | 0.022 97 | 0.020 93 | 0.017 81 | 0.012 74 |
| 14.00 | 0.109 62 | 0.076 24 | 0.059 67 | 0.042 93 | 0.033 40 | 0.022 82 | 0.020 91 | 0.017 97 | 0.012 37 |
| 14.50 | 0.106 00 | 0.073 48 | 0.057 69 | 0.041 87 | 0.033 47 | 0.023 13 | 0.020 68 | 0.017 89 | 0.012 05 |
| 15.00 | 0.102 57 | 0.070 78 | 0.055 46 | 0.040 54 | 0.033 13 | 0.023 56 | 0.020 09 | 0.017 42 | 0.011 66 |
| 15.50 | 0.099 29 | 0.068 24 | 0.053 13 | 0.038 92 | 0.032 27 | 0.023 85 | 0.019 08 | 0.016 52 | 0.011 12 |
| 16.00 | 0.096 19 | 0.065 92 | 0.050 90 | 0.037 09 | 0.030 97 | 0.023 83 | 0.017 73 | 0.015 27 | 0.010 44 |
| 16.50 | 0.093 31 | 0.063 81 | 0.048 93 | 0.035 19 | 0.029 37 | 0.023 38 | 0.016 21 | 0.013 82 | 0.009 65 |
| 17.00 | 0.090 64 | 0.061 86 | 0.047 26 | 0.033 38 | 0.027 67 | 0.022 47 | 0.014 70 | 0.012 33 | 0.008 84 |
| 17.50 | 0.088 14 | 0.060 04 | 0.045 87 | 0.031 81 | 0.026 02 | 0.021 17 | 0.013 35 | 0.010 98 | 0.008 10 |
| 18.00 | 0.085 77 | 0.058 35 | 0.044 69 | 0.030 58 | 0.024 56 | 0.019 64 | 0.012 27 | 0.009 87 | 0.007 49 |
| 18.50 | 0.083 47 | 0.056 80 | 0.043 62 | 0.029 73 | 0.023 36 | 0.018 08 | 0.011 54 | 0.009 05 | 0.007 05 |
| 19.00 | 0.081 28 | 0.055 40 | 0.042 61 | 0.029 20 | 0.022 49 | 0.016 70 | 0.011 14 | 0.008 54 | 0.006 78 |
| 19.50 | 0.079 21 | 0.054 11 | 0.041 64 | 0.028 90 | 0.021 95 | 0.015 66 | 0.011 04 | 0.008 30 | 0.006 67 |
| 20.00 | 0.077 27 | 0.052 89 | 0.040 69 | 0.028 67 | 0.021 67 | 0.015 01 | 0.011 16 | 0.008 29 | 0.006 67 |

$r_c/L \leq 0.1$, the $(qL)^2P(q)$ behavior becomes simpler than that at $r_c/L = 1$ and it resembles that of hollow rodlike micelles. At $r_c/L = 10$, $(qL)^2P(q)$ shows high-frequency oscillatory peaks at $qL < 6$. This is caused by highly symmetrical arrangement of the rods around the core of large $r_c$. Figure 11 shows plots of $P(q)$, instead of $(qL)^2P(q)$, against $qL$ for sea urchin molecules of $n = 32$. The size ratio $r_c/L$ is changed as 0.01, 0.1, 1, and 10. In the figure, $P(q)$ is drown separately at $y \geq 0$ and $y \leq 0$. At $r_c/L \leq 1$, drastic changes of $P(q)$ occur around $qL < 4$ when $y$ varies from ca. 1 to negative small values. This indicates that the sign of $\langle S^2\rangle_{app}$ changes from negative to positive. At $r_c/L = 10$, there are oscillatory damped curves with many peaks around $qL < 12$ and the initial slopes change from positive to negative at $y = 2.2$.

With eq 20–22 and 24, the apparent ms radius of gyration of sea urchin molecules $\langle S^2\rangle_{app}$ can be expressed in terms of $y$ as

$$\langle S^2\rangle_{app} = y^2\langle S^2\rangle_i + (1-y)^2\langle S^2\rangle_o + 2y(1-y)\langle S^2\rangle_{io} = y\langle S^2\rangle_i + (1-y)\langle S^2\rangle_o \quad (26)$$

since $2\langle S^2\rangle_{io} = \langle S^2\rangle_i + \langle S^2\rangle_o$. Thus it is shown that

$$\langle S^2\rangle_{app}/L^2 = [(r_c/L)^2 + (r_c/L) + 1/3] - [(2/5)(r_c/L)^2 + (r_c/L) + 1/3]y \quad (27)$$

For the rodlike star molecules, $w_i = 0$ ($y = 0$), $r_c/L = 0$, and we obtain that $\langle S^2\rangle_{app} = \langle S^2\rangle_{o,r_c/L=0} = (1/3)L^2$. For hollow rodlike star molecules, $y = 0$ and $\langle S^2\rangle_{app} = \langle S^2\rangle_o$. For the case that $w_i\nu_i + w_o\nu_o = 0$, it is shown that $y = \pm\infty$ and we obtain that $\langle S^2\rangle_{app} = +\infty$ or $-\infty$, depending on $y = +\infty$ or $-\infty$. For other cases, the values of $\langle S^2\rangle_{app}$ change from positive to negative with increase of $y$. The change occurs at $y = 1 + 9(r_c/L)^2/[6(r_c/L)^2 + 15(r_c/L) + 5] > 1$. Figure 12 shows this behavior in the form of $\langle S^2\rangle_{app}/L^2$ vs $y$ with $r_c/L$ changing from 0.5 to 20. A circle at $y = 0$ represents the value for rodlike star molecules. $\langle S^2\rangle_{app}/L^2$

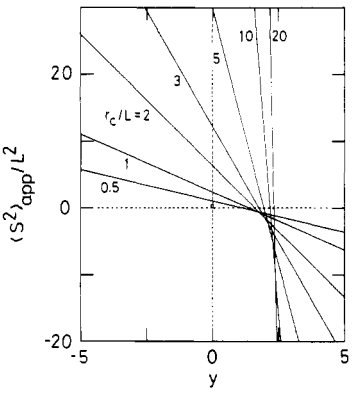


Figure 12. Variation of the reduced apparent mean-square radius of gyration $\langle S^2\rangle_{app}/L^2$ as a function of the weight-fraction refractive index increment of the core $y$ for sea urchin molecules with a given size ratio $r_c/L$. An unfilled circle at $y = 0$ represents the value for a rodlike star molecule.

is independent of n and the absolute value is larger at larger $r_c/L$. The former is in clear contrast to the molecule where the outer shell is constructed from the $n$ pieces of "Gaussian subchains". In this molecule, as will be described in detail in a forthcoming paper,[10] $\langle S^2\rangle_{app}/(R_G')^2$ depends strongly on $n$ and it shows similar behavior as in Figure 12 only at $n \to \infty$.

**Acknowledgment.** We thank Dr. K. Kajiwara for valuable discussion in course of the numerical computation of $P_o(q)$.

**Supplementary Material Available:** Lists of the algorithms (FORTRAN programs) used for calculating $P_o(q)$ and $P_{io}(q)$; List 1 is for the former for $n = 32$, for example, and List 2 is for the latter (12 pages). Ordering information is given on any current masthead page. The $P_o(q)$ algorithms for other $n$ values are available from the authors upon request.

## References and Notes

(1) Mazer, N. A. In *Dynamic Light Scattering*; Pecora, R., Ed.; Plenum: New York, 1985; Chapter 8.
(2) For example: Selb, J.; Gallot, Y. In *Developments in Block Copolymers 2*; Goodman, I., Ed.; Elsevier: London, New York, 1986.
(3) Recent reviews of neutral block copolymers have been given by: Burchard, M. *Adv. Polym. Sci.* **1983**, *48*, 1.
(4) Hirata, M.; Nemoto, N.; Tsunashima, Y.; Kurata, M. Proceedings of the 19th Yamada Conference on Ordering and Organization in Ionic Solutions, Kyoto, 1987.
(5) Rayleigh, J. W. *Proc. R. Soc. London, A* **1914**, *90*, 219.
(6) Neugebauer, T. *Ann. Phys. (N.Y.)* **1943**, *42*, 509.
(7) Debye, P. Lecture given at the Polytechnic Institute of Brooklyn, Brooklyn, NY, 1944; *J. Phys. Colloid Chem.* **1947**, *51*, 18.
(8) (a) Benoit, H. *J. Polym. Sci.* **1953**, *11*, 507. (b) Burchard, W. *Macromolecules* **1974**, *7*, 841.
(9) Benoit, H.; Froelich, D. In *Light Scattering from Polymer Solutions*; Huglin, M. B., Ed.; Academic: London, 1972.
(10) Tsunashima, Y.; Hirata, M.; Kurata, M. *Bull. Inst. Chem. Res., Kyoto Univ.*, in press.

# A Nearly Ideal Mixture of High Polymers

**C. A. Trask† and C. M. Roland***

*Chemistry Division, Code 6120, Naval Research Laboratory, Washington, D.C. 20375-5000.*
*Received April 21, 1988; Revised Manuscript Received July 6, 1988*

ABSTRACT: Determination of the mixing free energy of blends of *cis*-1,4-polyisoprene (PIP) and atactic poly(vinylethylene) (PVE) was attempted by estimation of the critical molecular weights of the components. Phase separation could not be induced, however, at the highest available molecular weights, indicating a Flory–Huggins interaction parameter for this mixture that is less than $1.7 \times 10^{-4}$. This remarkably low magnitude, in the absence of specific interactions, results from the small change in van der Waals energy upon mixing in combination with a close similarity in the liquid structure of the components. The exchange enthalpy of the blend is significantly increased when the PVE has syndiotactic microstructure, resulting in immiscibility with PIP at moderate molecular weights. The glass transition of the PIP/PVE blend was observed to be unusually broad in the presence of a high concentration of PVE. This breadth is unrelated to phase segregation effects but likely reflects differences between components in the free volume necessary for segmental mobility.

## Introduction

Ideal solutions result from the random mixing of molecules that have the same size and shape and in which the intermolecular forces between pairs of like segments of each type, as well as between unlike segments, are all equivalent. The mixing enthalpy associated with dispersive interactions (arising from correlation between charge fluctuations) favors phase segregation. For macromolecules, in which the combinatory mixing entropy is small, this usually restricts miscibility to only those mixtures in which the components chemically interact. This combinatory entropy is not negligible however and in blends of *cis*-1,4-polyisoprene and atactic poly(vinylethylene) has been shown to be sufficient to effect miscibility as a result of the small enthalpy change accompanying mixing.[1,2] The magnitude of the dispersion energy can be described by a series whose leading term corresponds to the well-known London equation[3]

$$E_{ij} = -\tfrac{3}{4} I_{ij} \alpha_i \alpha_j r^{-6} \tag{1}$$

where $\alpha_i$ is the polarizability of the $i$th molecule or chain unit, separated by $r$ from the $j$th unit, and $I_{ij}$ is approximately equal to the ionization potential of the species. If no alterations of the local liquid structure accompany mixing, the Flory–Huggins interaction parameter, $\chi_{ij}$, describing the enthalpy and noncombinatory entropy contributions to the free energy, can be directly related to the dispersion interaction energy according to[4]

$$\chi_{ij} = (E_{ij} - E_{ii}/2 - E_{jj}/2)/RT \tag{2}$$

A negligible change of van der Waals energy upon mixing is primarily a consequence of similarity in the respective polarizabilities of the blend components. The ideal combinatory entropy change, per lattice (or chain unit) volume, is given for a two-component mixture by[4]

$$\Delta S = -R(\phi_i/N_i \ln \phi_i + \phi_j/N_j \ln \phi_j) \tag{3}$$

where $\phi$ is volume fraction, $R$ the gas constant, and $N$ the degree of polymerization. By increasing $N$, this entropy can be diminished to an extent whereby the dispersive interaction energy is sufficient to effect phase separation. The critical point, or minimum on the spinodal curve, defines a value of the Flory–Huggins interaction parameter below which the system is miscible at all concentrations of the components. The composition at the critical point is deduced by equating the third derivative of the free energy with respect to concentration to zero and solving to obtain[5]

$$\phi_i^* = N_j^{1/2}/(N_i^{1/2} + N_j^{1/2}) \tag{4}$$

with the corresponding critical value of the interaction parameter then given by

$$\chi^* = V_R/2[(V_i N_i)^{-1/2} + (V_j N_j)^{-1/2}]^2 \tag{5}$$

† Geo-Centers, Inc., Fort Washington, MD.

0024-9297/89/2222-0256$01.50/0 